A Heat and Mass Transfer Study—Analysis of Continuous Processes for the Coloration of Polyester Fabric. II. Modelling and Characteristics of the (Polyester) Fabric Heating*

SAMI E. AKAOUI,† *School of Textiles, North Carolina State University, Raleigh, North Carolina 27650*

Synopsis

First it is shown how the equations used for the numerical solution of the transient heat transport to a body can be reduced to the simple transport model (of Paper I), which is commonly used in the textile literature for estimating the heat transfer coefficient (h) of the various fabric heating equipment. During the thermal treatment of a fabric that can be approximated by a geometrically stable homogeneous plate, the simple transport model should not be used for calculating h in cases of high heating rate equipment (e.g., direct contact units) instead; the numerical solution should be used. For a fabric that becomes geometrically unstable during a thermal treatment, like polyester knits, the h value obtained by fitting the numerical solution to the fabric heating rate measurement becomes an apparent coefficient that is the function of the fabric thermal history rather than the equipment heating efficiency. However, if the objective of the modelling is to represent the geometrically unstable fabric heating rate, the simple transport expression is a viable alternative to an otherwise intricate model.

INTRODUCTION

In this part of the investigation of the heat and mass transfer during the polyester fabric coloration, the reasons for the convergence and deviation of the simple model for a fabric heating [as expressed in eq. (22) in Paper I] relative to the more correct numerical analysis solution are analyzed. This is followed by a brief examination of the limitations of heating a solid body by forced convection using gases, and a review of the range of values of the heat transfer coefficients for the different possible heating systems, as well as for the industrial (practical) textile fabric heating equipment. A commentary is made on the calculations used for the estimation of the heat transfer coefficient values adopted by the international textile literature for high heating rate equipment. The temperature distribution inside a model fabric (knitted polyester) under different heat transfer coefficient values is demonstrated, assuming the homogeneous plate approximation of the fabric and using the numerical solution. A correlation between the fiber (inside the fabric) heat transfer coefficient (h_f), and the fabric heat transfer coefficient (h_F) is derived and graphically presented. The correlation demonstrates the limited accessibility of the fiber surface area for heat transfer. A comparative study is then made for the heating characteristics of

* Part I is Ref. 16.

† Candidate for Ph.D. degree in Fiber and Polymer Science.

Journal of Applied Polymer Science, Vol. 27, 4713–4733 (1983)
 CCC 0021-8995/124713-21$03.10

the three coloration processes under investigation: thermosol, high temperature steaming (HT steaming), and heat transfer printing (HTP). Finally, the importance of the HTP blanket permeability is pointed out as a practical heat transfer theory application exercise.

A GENERAL EXPRESSION FOR THE NUMERICAL SOLUTION OF THE HEAT TRANSMISSION TO A BODY—THE THREE BASIC GEOMETRIES

Equation (22) (derived in Paper I) is a simple expression for the 1-dimensional heating of a body of any geometry that can be characterized by a specific area of heat transport (A_s). The body is initially at temperature T_0 and is placed at time $t = 0$ within a heat source at temperature T_∞; the body temperature (T) in this equation is assumed to be at all times uniform and equal to the mean body temperature (T_m):

$$\frac{A_s \cdot h_T \cdot t}{C_T} = \ln \frac{T_\infty - T_0}{T_\infty - T_m} \qquad \text{(22—Paper I)}$$

$$A_s = \frac{m}{\rho \cdot \delta} \qquad \text{(23—Paper I)}$$

In eq. (22) h_T is the overall heat transfer coefficient that is also denoted by h for simplicity, and C_T is the specific heat capacity of the body. Equation (23) is an expression for the specific heat transfer area (A_s) for three basic body geometries: semiinfinite plate ($m = 1$), semiinfinite cylinder ($m = 2$), and sphere ($m = 3$)—ρ is the density of the body, and δ is a characteristic geometrical dimension. In the case of the plate, δ equals half the plate thickness; in the case of the cylinder or sphere δ equals the radius. By substituting from eq. (23) in (22), Equation (24) results:

$$\frac{m \cdot h_T \cdot t}{\rho \cdot \delta \cdot C_T} = \ln \frac{T_\infty - T_0}{T_\infty - T_m} \qquad \text{(24—Paper I)}$$

The limitations of eq. (22) [or (24)] have been discussed in Paper I of this investigation.

An expression analogous to eq. (24) can be derived for representing the 1-dimensional heating of the three basic geometries (plate, cylinder, and sphere). This expression does also account for the temperature distribution inside the body. This is achieved by dividing the body into compartments, and then obtaining the heating rate of each compartment from an elemental energy balance; the generated equations are then solved numerically, and the results are conveniently graphed, as in Refs. 1 and 2, using the dimensionless parameters $(T_\infty - T)/(T_\infty - T_0)$, $(\alpha \cdot t/\delta^2)$, and $(k/h \cdot \delta) - \alpha$ and k are the body thermal diffusivity and thermal conductivity, respectively. Graphs are plotted for the different geometries, and for each geometry a family of curves is generated for the temperature (T) at different locations (x/δ) in the body.

Let us consider a semiinfinite plate of thickness (2δ), a cylinder of infinite length and radius (δ), and a sphere of radius (δ). By dividing these three basic geometries by an equal number of partitions (N), resulting in a total of N + 1 compartments, with the surface and center compartments having half the width

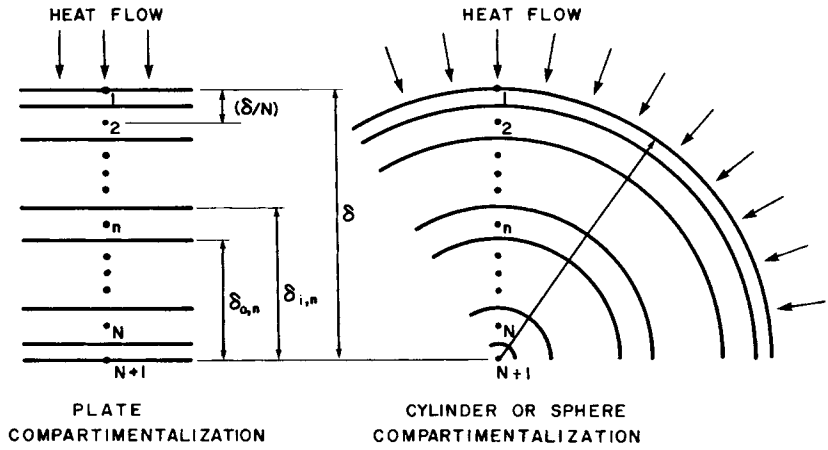

Fig. 11. Body compartimentalization for numerical analysis.

of a compartment in the body interior—as shown in Fig. 11*—and then performing the energy balance on each compartment, eq. (37) is obtained. Equation (37) represents the specific heating rate [thermal units/(unit mass · unit time)] in each compartment (n) for the three geometries:

$$C \cdot \frac{dT_n}{dt} = k \cdot \left[A_{i,n} \cdot \frac{(T_{n-1} - T_n)}{(\delta/N)} - A_{0,n} \cdot \frac{(T_n - T_{n+1})}{(\delta/N)} \right], \qquad n = 1, 2, \ldots, N, N+1 \quad (37)^{\dagger}$$

heat accumulation

= difference between heat flowing in and out of compartment (37′)

$$A_{i,n} = \frac{m \cdot \delta_{i,n}^{m-1}}{\rho \cdot (\delta_{i,n}^m - \delta_{0,n}^m)} = \left(\frac{m}{\rho \cdot \delta}\right) \cdot \frac{r_{i,n}^{m-1}}{(r_{i,n}^m - r_{0,n}^m)} \quad (38a)$$

$$A_{0,n} = \frac{m \cdot \delta_{0,n}^{m-1}}{\rho \cdot (\delta_{i,n}^m - \delta_{0,n}^m)} = \left(\frac{m}{\rho \cdot \delta}\right) \cdot \frac{r_{0,n}^{m-1}}{(r_{i,n}^m - r_{0,n}^m)} \quad (38b)$$

$$\delta_{i,n} = \delta \cdot r_{i,n} \quad (39a)$$

$$\delta_{0,n} = \delta \cdot r_{0,n} \quad (39b)$$

$$r_{i,n} = 1 - \frac{n-1}{N} + \frac{1}{2N} \qquad n = 2, 3, \ldots, N+1 \quad (40a)$$

$$r_{0,n} = 1 - \frac{n-1}{N} - \frac{1}{2N} \qquad n = 1, 2, \ldots, N \quad (40b)$$

As for eq. (24), in eq. 38 the value of m is 1 for the plate, 2 for the cylinder, and 3 for the sphere. The quantities $A_{i,n}$ and $A_{0,n}$ are the specific areas of transport in and out of compartment (n), respectively. At the body interface where the value of n is 1, $r_{i,n} = 1$, T_{n-1} is equivalent to the heat source temperature (T_∞), and $A_{i,1}$ should be multiplied by the term $h \cdot (\delta/N)/k$. At the center of the body where $n = N + 1$, $r_{0,n} = 0$, and, accordingly, $A_{0,N+1} = 0$—no heat can leave the

* Figures 1–10 appear in Paper I (Ref. 16.).

† Equations (1)–(36) appear in Paper I (Ref. 16).

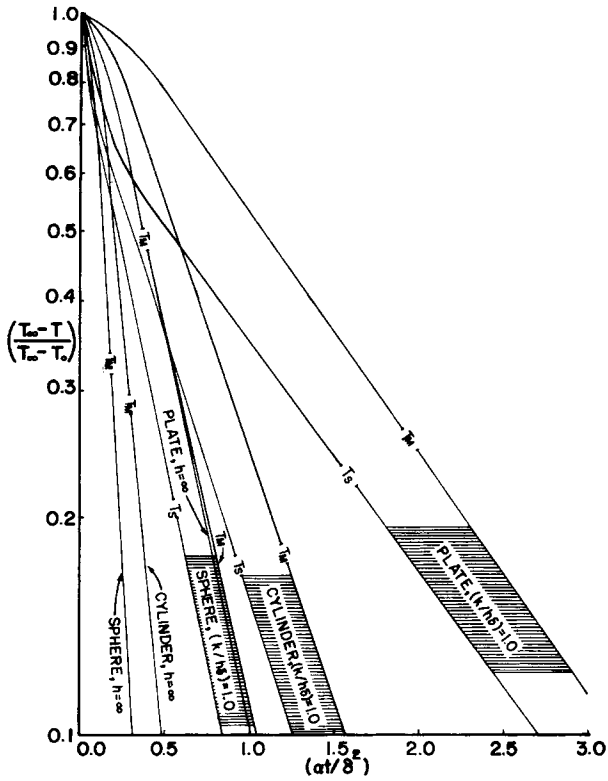

Fig. 12. The heating rate of the three basic geometries: semiinfinite plate, semiinfinite cylinder, and sphere at $(k/h\delta) = 0$ and 1.

center compartment. Note that T_{N+1} and T_1 are equivalent to T_M and T_S—the body center and surface temperatures, respectively—and that $A_{i,1}$ is the equivalent of A_s in eq. (22).

By substituting as just mentioned, the heating rate at the center of the three basic geometries is readily obtained.

$$\left.\frac{dT_{N+1}}{dt}\right|_{\text{plate}} = 1 \cdot \left(\frac{\alpha}{\delta^2}\right) \cdot 2N^2 \cdot (T_N - T_{N+1}) \tag{41}$$

$$\left.\frac{dT_{N+1}}{dt}\right|_{\text{cylinder}} = 2 \cdot \left(\frac{\alpha}{\delta^2}\right) \cdot 2N^2 \cdot (T_N - T_{N+1}) \tag{42}$$

$$\left.\frac{dT_{N+1}}{dt}\right|_{\text{sphere}} = 3 \cdot \left(\frac{\alpha}{\delta^2}\right) \cdot 2N^2 \cdot (T_N - T_{N+1}) \tag{43}$$

Equations (41), (42), and (43) show that, for the same temperature difference $T_N - T_{N+1}$, a correlation exists between the heating rates of the three body geometries under consideration: the heating rate of the sphere center is three times that of the plate which is half that of the cylinder. Accordingly, the time necessary for the plate center to reach a certain temperature (T_M) will be (beyond the initial heating stage) approximately three times larger than that needed for the sphere and twice that for the cylinder—as can be demonstrated from Figure 12. This is more so during the advanced stages of heating the body $[(T_\infty - T)/$

$(T_\infty - T_0) > 0.6$ in Fig. 12] and under low heat transfer coefficients, or more generally at higher values of the ratio $(k/h \cdot \delta)$. During the initial stages of heating a body, the heat transmission is limited to the body skin, and the body geometry effects on the heating rate are negligible.

At low heat transfer coefficient values, or at larger magnitudes of the dimensionless parameter $(k/h\delta)$, the rate-determining step becomes the heat transfer from outside to inside the body, or the heating rate at the interface, which can be readily derived by making the required substitutions in eq. (37):

$$\left.\frac{dT_1}{dt}\right|_{\text{plate}} = 1 \cdot \left(\frac{\alpha}{\delta^2}\right) \cdot \frac{N}{(1 - r_{0,1}^1)} \cdot \left[\frac{1}{N \cdot (k/h\delta)} \cdot (T_\infty - T_1) - (T_1 - T_2)\right] \quad (44)$$

$$\left.\frac{dT_1}{dt}\right|_{\text{cylinder}} = 2 \cdot \left(\frac{\alpha}{\delta^2}\right) \cdot \frac{N}{(1 - r_{0,1}^2)} \cdot \left[\frac{1}{N \cdot (k/h\delta)} \cdot (T_\infty - T_1) - r_{0,1} \cdot (T_1 - T_2)\right] \quad (45)$$

$$\left.\frac{dT_1}{dt}\right|_{\text{sphere}} = 3 \cdot \left(\frac{\alpha}{\delta^2}\right) \cdot \frac{N}{1 - r_{0,1}^3} \left[\frac{1}{N \cdot (k/h\delta)} \cdot (T_\infty - T_1) - r_{0,1}^2 \cdot (T_1 - T_2)\right] \quad (46)$$

Under such conditions (low h values), the temperature distribution inside the body tends to be more uniform, and $T_1 - T_2$ in eqs. (44), (45), and (46) approaches zero. Furthermore, by considering the body made of one compartment only, since the body temperature distribution is approaching uniformity, the above equations are reduced to the differential form of eq. (22), which explains the agreement between the numerical analysis and eq. (22) in Figure 10 of Paper I.

CHARACTERISTICS OF THE POLYESTER FABRIC HEATING

Forced Convection by Gases

At this stage it should be mentioned that heat convection by gases is limited by the maximum velocities obtainable at atmospheric pressure; a gas velocity cannot exceed the speed of sound. The velocity of sound in a gas increases as the temperature is increased, for an ideal gas,[3]

$$v_s = 331.5 + 0.607T \quad (47)$$

where v_s = sound velocity (m/s) and T = gas temperature (°C). From eq. (47) the maximum theoretical velocity that a gas can reach at 210°C is 459 m/s. Empirically, the following correlation relates the heat transfer coefficient to the gas velocity in forced convection, especially air and superheated steam[2]:

$$h = 2.446\ (3.05\ v)^{0.8} \quad (48)$$

where v = gas velocity (m/s) and h = heat transfer coefficient by the forced convection (W/m^2 · °K).

Hypothetically, the maximum heat transfer coefficient possible by forced gas convection is [from eq. (48)] 800 W/m^2 · °K. Obviously, such high heat transfer coefficients cannot be practically implemented in industrial heating equipment by forced convection with gases. The following section reviews the practical

TABLE V
Range of Heat Transfer Coefficient Values for Different Heating Modes

Heating mode	Heating medium	h (W/m^2·°K)	Ref.
Forced convection	Flowing gases	12–280	1
	Flowing liquids	170–5,670	1
	Flowing liquid metals	5,670–283,000	1
Natural convection	Gases	5–28	1
Phase transformation	Boiling liquids	320–283,000	1
	Condensing vapors	2,830–28,300	1
Conduction	Direct contact	230–2,300	4
Radiation[a]	Infrared radiation	0–∞	—

[a] Note:

$$h_R = F \cdot E \cdot \sigma \frac{(T_\infty^4 - T_S^4)}{(T_\infty - T_S)} \qquad (18'\text{—Paper I})$$

In the above expression h_R is the heat transfer coefficient due to radiation, F the geometric factor, E fabric emissivity, σ the Stefan–Boltzman constant, and T_∞ is the radiating element temperature, and T_S is the fabric surface temperature. Note that the temperature in eq. (18′) has to be in °K.

values of heat transfer coefficients of textile heating equipment for thermosol units.

Order of Magnitude Values of Heat Transfer Coefficients in Practical Heating Systems

Values of heat transfer coefficients for different heating modes and textile heating equipment are listed in Tables V and VI,* respectively. From Table V one can see that high heat transfer coefficients (or rapid heating of a solid body) can be achieved by using forced convection with liquid metals, phase transformation in boiling liquids, or radiation. Heating with liquid metals is rather expensive and requires special handling in cases where hazardous vapors are evolved—most of the metallic elements involved in the formation of low melting point alloys have been proven to constitute real hazards to the human health, e.g., lead, cadmium, mercury, etc. Boiling liquids are easier to control under atmospheric pressure; however, when high heating temperatures are desired, say 200°C, for continuous processing of a material, pressurizing liquids in order to reach higher boiling points results in serious sealing problems, especially if the liquid vapor is harmful. On the other hand, when using a boiling liquid in order to heat a material such as a textile fabric, possible adverse effects that the liquid may have on the heated substance should be taken into consideration, as well as the total costs of removal and recovery (when needed) of the liquid from the fibrous structure after the heating process. This leaves water as the foremost candidate among liquids for safe and economical heating of the fabric.

Infrared radiation heating is rather safe and offers the widest range of heat transfer coefficients. Unfortunately, close control of the processed material temperature under high heat transfer coefficient values can be difficult. This is because of the high radiating element temperatures that are necessary in order to reach high heat transfer coefficient values (see footnote of Table V), which

* Tables I–IV appear in Paper I (Ref. 16).

TABLE VI
Heat Transfer Coefficient Values For Different Fabric Heating Equipment

Equipment type[5]	Average reported fabric heating times[5] (s)	h (W/m^2·°K)[a] As in Ref. 5 and using eq. (5)	Using eq. (22)	Obtained from numerical analysis[1]
Hot flue:				
Convective heat transfer with low velocity hot air circulation	30–60	30	20	20
Tenter frame:				
Convective heat transfer with high velocity hot air circulation	5–20	230–60[b]	120–60	150–80
Perforated cylinders:				
Convective forced hot air circulation combined with conductive heat transfer	3	400	400	800
Contact cylinders:				
Conductive heat transmission	3, (4)[c]	300	300	600

[a] For one-sided fabric ($\rho'_F = 0.3$ kg/m^2) heating $A_s = 1/\rho'_F$, $\delta_F = 1.25 \times 10^{-3}$ m, and for two-sided heating $A_s = 2/\rho'_F$, $\delta_F = 0.625 \times 10^{-3}$ m. In all cases $T_\infty = 210$°C, $T_0 = 20$°C, T_m (or T_S) = 200°C, and the time in column 2 is assumed to be $t_{0.9}$.

[b] The value reported in the original article is typographically incorrect.

[c] Calculations in columns 4 and 5 in the table are based on $t_{0.9} = 4$ s.

increases the risk of overheating the material being processed beyond the required temperature. Expensive instrumentation may be necessary in order to attain a satisfactory level of temperature control. Thus, choosing a heating system requires thorough consideration of the total of the equipment and operating costs including costs of compliance to the environmental and safety regulations.

Table VI shows the heating systems that are industrially practical for the fabric heating during the thermosol operation. Hauben and Pabst[5] obtained the heat transfer coefficient values in Table VI from measurements of the heating rate of polyester textile fabrics in the different types of heating units described in column 1 of Table VI. An approximation of the fabric mean temperature (T_m) is usually obtained by recording the reading of a thermocouple inserted between two layers of the fabric. When two layers of a fabric sandwich are heated from both sides with a thermocouple in between, the specific area of heat transfer (A_s) becomes the reciprocal of the fabric areal density (ρ'_F). Now, if the temperature distribution throughout the fabric cross section is assumed uniform, eq. (22) becomes the expression used in literature[5,6] for representing the fabric heating, i.e.,

$$\frac{h_F \cdot t}{\rho'_F \cdot C_F} = \ln \frac{T_\infty - T_0}{T_\infty - T_m} \qquad \text{(5—Paper I)}$$

Conveniently enough, the same equation can be used for expressing the heating of a fabric from one side if the fabric is insulated from its other side. These conditions are practically achieved by the direct contact heating of a fabric over a cylinder. Hauben and Pabst[5] used eq. (5) for estimating the equipment heat transfer coefficient from fabric heating rate measurements. However, in Ref.

5 a common engineering practice for representing the heat transfer coefficient is used: Instead of doubling the specific area of heat transfer when the fabric is heated from both sides, it is the heat transfer coefficient value that is doubled. Of course, this practice does not affect the fabric heating rate as expressed in eq. (5), but it would be more reasonable to change the variables—A_s and h—in eq. (22) and (5) such that a closer representation of reality is assumed. The heat transfer coefficient in this case should remain the parameter that represents the ease of heat flow from the heat source to the fabric "surface," and heating the fabric (that is approximated by a "homogeneous plate") from both sides in a heat source should not alter the characteristics of the heat transfer between the source and the body surface.

The heat transfer coefficient values in Table VI can be reproduced (with one- or two-digit accuracy) by using eq. (22) with the corresponding times ($t_{0.9}$) in column 2. It is important to note that hot flue and tenter frame units can be used for either one- or two-sided fabric heating, but during direct contact heating of the fabric, as in the cylinder units, the fabric is heated from one side only at any one time, except as the fabric moves from one cylinder to another, which is a very short time interval compared to the time a differential fabric area (dA) spends on one cylinder surface. Therefore, for the sake of simplicity, during direct contact heating of a fabric, the later process is considered as a one-sided "plate" heating. On the other hand, according to this investigation, A_s in eq. (22) equals $(1/\rho_F')$ for one-sided fabric heating [as in eq. (5)] and A_s has to be equated to $(2/\rho_F')$ for the two-sided fabric heating. In this later case and according to Ref. 5, A_s remains unchanged and h is doubled instead. As a result, the h values reported in column 3 of Table VI do not have the same interpretation as in this study (columns 4 and 5). Bearing that in mind, the time values in Table VI are used to produce the heat transfer coefficients in columns 3, 4, and 5. For example, hot flue units require an average of 30 s and 60 s for two-sided and one-sided fabric heating time ($t_{0.9}$), respectively. Now, by proper substitution in eq. (22), as follows: $A_s = 1/\rho_F'$ (for one-sided fabric heating), $\rho_F' = 0.3$ kg/m^2, $C_F = 1.38 \times 10^3$ J/kg · °K, $t_{0.9} = 60$ s, and $(T_\infty - T_0)/(T_\infty - T_m) = (210 - 20)/(210 - 200)$, one obtains an h value of 20 W/m^2 · °K (column 4). The same h value is obtained for the two-sided fabric heating where $A_s = 2/\rho_F'$ and $t_{0.9} = 30$ s. Note that, in this later case, according to Ref. 5, h is 40 W/m^2 · °K—as obtained by using eq. (5) with $t_{0.9} = 30$ s. The h value in column 3 of Table VI (for hot flue units) is the arithmetic average of 40 and 20 W/m^2 · °K—the two-sided and one-sided fabric (heating) heat transfer coefficients, respectively. Similarly, for the tenter frame units, 5–20 s is the heating time range for two-sided and the slowest one-sided fabric heating, respectively. These time values are used for generating the heat transfer coefficients in columns 3, 4, and 5.

The minimum time ($h = \infty$) for the fabric under consideration ($\rho_F' = 0.3$ kg/m^2) to reach a T_m of 200°C is almost 2.2 s [using eq. (36) in Paper I] for two-sided heating ($\delta_F = 0.625 \times 10^{-3}$ m), and 8.7 s for one-sided heating ($\delta_F = 1.25 \times 10^{-3}$ m). The fact that it takes an average of 3 s for the one-sided fabric heating in the perforated cylinder unit (or 4 s for direct contact cylinders) is attributed to a rather fabric surface temperature T_S measurement—and not T_M or T_m—that was made for estimating the times in column 2 of Table VI. (Figure 13 demonstrates the possible differences between the T_S, and T_M temperatures.) If the fabric is approximated to a homogeneous plate, correct theoretical application

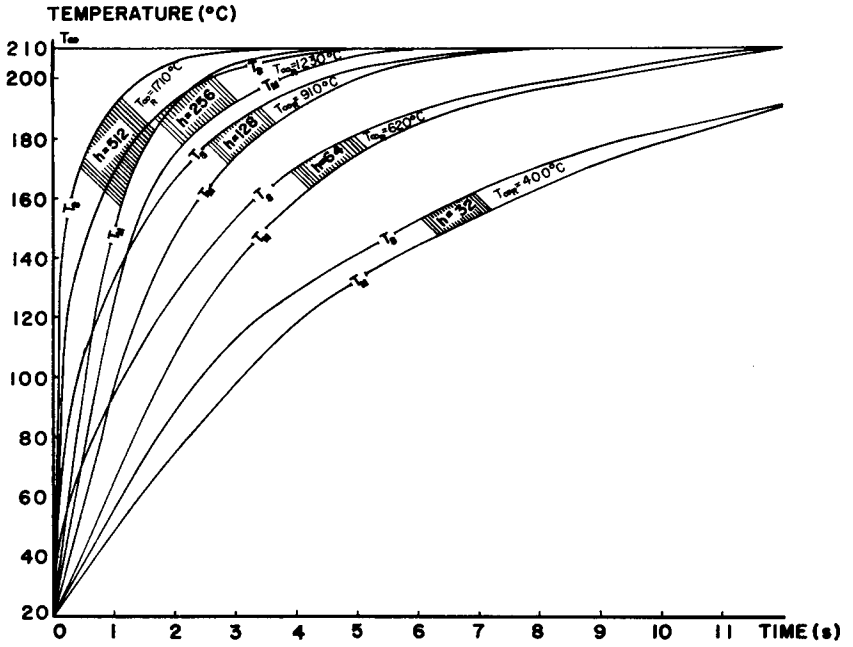

Fig. 13. Fabric heating rate under different heat transfer coefficients: h = overall heat transfer coefficient ($W/m^2 \cdot °K$); T_M = fabric midplane temp (°C); T_S = fabric surface temp (°C); $T_{\infty R}$ = equivalent radiating plates temp (°C).

of such a model requires one not to use eq. (22) (in its different forms) for high heat transfer coefficient magnitudes that result in a highly nonuniform temperature gradient inside the fabric, thus violating one of the basic assumptions on which eq. (22) is based. In Table VI, the plate approximation model of the fabric is used in Ref. 5 in order to estimate heat transfer coefficients from the heating time ($t_{0.9}$) measurements at high h magnitudes, or low $t_{0.9}$ values; consequently, the calculated h coefficients for the high heating rate units are underestimated. For instance, for direct contact heating using cylinders, for $t_{0.9}$ = 4 s, ρ'_F = 0.3 kg/m^2, $C_F = 1.38 \times 10^3$ J/kg · °K, and $(T_\infty - T_0)/(T_\infty - T_m)$ = (210-20)/(210-200), h as calculated from eq. (22) [or (5)] yields 300 W/m^2 · °K, whereas using the more correct numerical analysis graphical solution[1] results in an h value twice as much: 600 W/m^2 · °K. This latter value is obtained by assuming that the fabric thermal diffusivity (α_F) is 2.0×10^{-7} m^2/s (α_F is not significantly affected by changes in ρ'_F[7]) and that the fabric thickness is 1.25×10^{-3} m—a reasonable assumption, since for (ρ'_F) = 0.24 kg/m^2, the fabric thickness is around 10^{-3} m. This extent of deviation between the h values obtained from eq. (22) and the numerical analysis solution is to be expected, and is similar to the deviations previously demonstrated by the model fabric in this study for high heat transfer coefficients (see Fig. 10 in Paper I).

The homogeneous plate approximation of the fabric with correct application of the model (using the numerical analysis solution at high h values) would be a satisfactory representation of the heating process of a geometrically stable fabric. However, one of the most common types of polyester fabric involves the texturing and knitting of the yarn. This fabric demonstrates a significant geo-

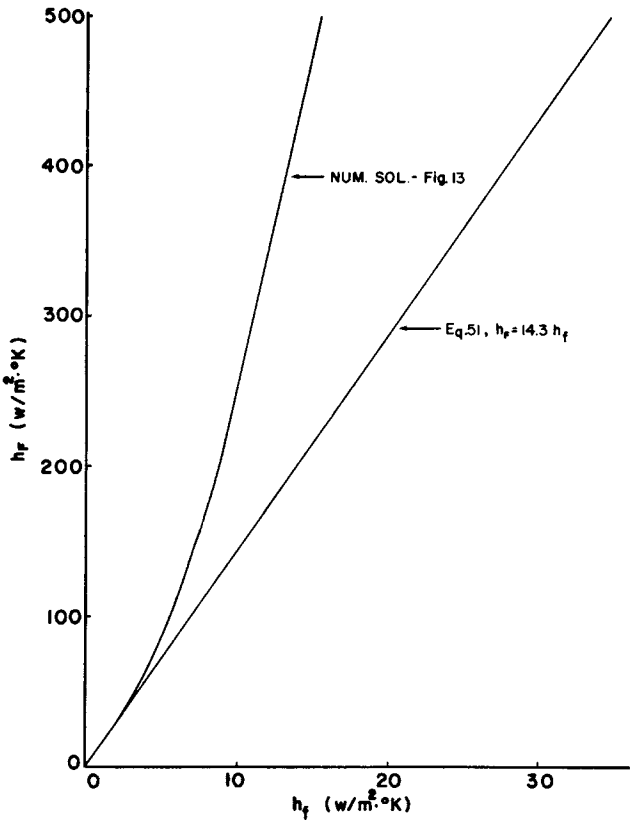

Fig. 14. Relation between fabric and fiber-in-fabric heat transfer coefficients.

metrical instability at high temperature treatments, say at 210°C, that is manifested by the degradation of the fabric hand properties.[8] Under such circumstances, the capacity of the homogeneous and geometrically stable plate model for representing the fabric heating requires further investigation. This is done in a separate section.

Temperature Distribution in Fabric at Different Heat Transfer Coefficients

Figure 13 illustrates, using graphical solution of numerical analysis,[1] a model polyester fabric (with physical properties as in Table XII) heating rate under different heat transfer coefficients. As expected, the higher the heat transfer coefficient is, the more nonuniform the fabric heating becomes, i.e., the larger is the difference between the fabric surface temperature and the fabric midplane temperature—especially at the early stages of the fabric heating. The variables in Figure 13, temperature (T), time (t), and heat transfer coefficient (h_F), can be readily converted to the more useful dimensionless variables: $(T_\infty - T)/(T_\infty - T_0)$, $(\alpha_F \cdot t/\delta_F^2)$, and $(k_F/h_F \cdot \delta_F)$—thus making Figure 13 readily applicable to other types of fabric having a different set of physical parameters. For example, by subtracting T from T_∞ (210°C) and dividing the result by $T_\infty - T_0 = 210 - 20$ (°C), the ordinate variable T in Figure 13 is transformed to the di-

TABLE VII
Equivalent Radiating Element Temperature

$T_{\infty R}$(°C)[a]	$h_{210°C}$	$h_{20°C}$	$\bar{h}_R$[b]	$h_{\bar{T}}$[c]	h (Fig. 14)
400	42	28	35	34	32
620	76	56	66	65	64
910	145	117	131	130	128
1230	264	225	245	243	256
1710	548	488	518	516	512

[a] $T_{\infty R}$ = radiating element temperature that would produce the heating rate curves as in Fig. 13 for the corresponding h values as in column 6.

[b] $\bar{h}_R = (h_{210°C} + h_{20°C})/2$ (W/m^2·°K).

[c] $h_{\bar{T}}$ = the radiative heat transfer coefficient at the arithmetic average temperature between the final fabric desired temperature (210°C) and the initial fabric temperature (20°C), $\bar{T}$ = 115°C, using eq. (18).

mensionless temperature parameter $(T_\infty - T)/(T_\infty - T_0)$, which varies between 1.0 and 0.0. Similar conversions can be performed on the other two variables h_F and t—as in Figure 12.

The results in Figure 13 show that the hot flue type of heating (low h_T values) will produce a more uniform heating in the fabric cross section, though the heating time is relatively long—as shown in Table VI. Contact cylinder or perforated cylinder type of heaters heat the fabric very rapidly, but the difference between the fabric surface temperature and the fabric center becomes very high.

In Table VII, for each value of h in Figure 13 and a desired final temperature (T_m), a corresponding radiation temperature, as in eq. (18) (see footnote of Table V), is estimated—similar values have been obtained in Table I of Paper I. The radiation temperature ($T_{\infty R}$) is the temperature of two infrared radiating plates that are in parallel and on both sides of the fabric surface.

Heat Transmission to Fibers Inside the Fabric

At this stage it is possible to analyze the heat transfer to the individual fibers inside the fabric and compare it to the heat transfer to the fabric. From eq. (24) the time needed for the mean fabric temperature to reach 199°C (T_m) when the heating medium is at 210°C (T_∞) can be readily calculated:

$$(t_{0.9})_F = \frac{\rho_F \cdot C_F}{2h_F} \ln \frac{T_\infty - T_0}{T_\infty - T_m} \tag{49}$$

This is how long it takes the fabric to heat up to T_m for a specific h_F value. Now, the $(t_{0.9})_F$ value can be used to estimate the heat transfer coefficient to the fibers inside the fabric. From eq. (24) with the proper substitutions

$$h_f = \frac{\rho_f \cdot (R_f/2) \cdot C_f}{(t_{0.9})_F} \ln \frac{T_\infty - T_0}{T_\infty - T_m} \tag{50}$$

It has to be noted that $(t_{0.9})_f = (t_{0.9})_F$ since the fabric temperature heating rate is determined by measuring the fibers (in the fabric) temperature. In eq. (50), (h_f) is an average heat transfer coefficient of the fibers in the fabric. This parameter will indicate the efficiency of heating the fibers inside the fabric. By dividing eq. (49) by eq. (50) and rearranging, one obtains

TABLE VIII
Relation between Heat Transfer Coefficients of Fabric (h_F) and Fiber in Fabric (h_f)

h (W/m^2·°K)		
h_F	h_f [eq. (51)]	h_f (Fig. 13)
32	2.2	2.1
64	4.5	4.1
128	8.9	6.6
256	17.8	10.1
512	35.7	15.8

$$\frac{h_F}{h_f} = \frac{\rho_F' \cdot C_F}{\rho_f \cdot R_f \cdot C_f} \tag{51}$$

for the fabric under investigation eq. (51) becomes

$$h_F = \frac{(0.24)(1.38)}{(1380)(10^{-5})(1.67)} = 14.35h_f \tag{51'}$$

Equation (51) shows that the heat transfer coefficient to the fiber (h_f) is directly proportional to the fabric heat transfer coefficient (h_F), but about 14 times smaller than h_F. This is mainly due to the fact that the fiber specific area of heat transfer ($A_f = 2/\rho_f \cdot R_f$) is about 17 times larger than the plane fabric specific area ($A_F = 1/\rho_F \cdot \delta_F$); but the fiber in the fabric does not heat as fast as expected because of the limited fiber surface accessibility to the heat source.

Table VIII shows the variation in h_f with h_F using eq. (51), and also from values of temperatures T_m = 199°C, and time ($t_{0.9}$) obtained from Figure 13, the numerical analysis solution, and then eq. (50) is used to estimate h_f. Since the h_f values are low, or more specifically the ratio ($k_f/h_f\delta_f$) is high, eq. (50) yields accurate results as discussed above. Figure 14 illustrates the relation between the two heat transfer coefficients.

Analysis of the Heating Rate in Different Polyester Coloring Processes

Equation (22) can be used to compare the heating efficiency of different fabric heating units. This efficiency is really the capability of the equipment to transmit heat to the fabric, which is reflected by the fabric heating rate ($\dot{Q}$) at a given temperature gradient ($T_\infty - T_m$); ($\dot{Q}$) is related to the heat transfer coefficient (h_T) as follows:

$$\dot{Q} = h_T(T_\infty - T_m) \tag{52}$$

The heating efficiency of different fabric heating equipment can be quantitatively estimated by recording the time it takes each unit to heat the same fabric to a reference temperature, say until T_M reaches 90% of the final desired temperature T_∞, and $T_m = (T_{\text{LMT}})$ with $T_S = T_\infty$; then from eq. (22) it can be readily shown that the equipment heat transfer coefficient (say, for unit 1 or 2) is inversely proportional to the reference heating time ($t_{0.9}$)—the time it takes the fabric to reach the reference temperature (T_m) just mentioned:

$$\frac{h_1}{h_2} = \frac{1/(t_{0.9})_1}{1/(t_{0.9})_2} \tag{53}$$

TABLE IX
Fabric Heating Rate in Lab HT Steamers and Benz Units

T_∞ (°C)	Lab HT steamer[a] ($t_{0.9}$) (s)	Benz unit[b] ($t_{0.9}$) (s)	h_s/h_A[c]	Ref.
210	70	60	0.86	9
180	25	30	1.2	10
180	26.5	34	1.28	11
180	23	28	1.2	12
180	8	12	1.5	13

[a] The fabric is fed into an atmosphere of 100% superheated steam with low steam circulation.
[b] Benz heating units operate with a high velocity circulation of hot air in the unit. This simulates the operation of a conventional thermosol unit.
[c] $h_s/h_A = (1/t_{0.9})_s/(1/t_{0.9})_A$—as in eq. (53).

In the above equation, h_1 and h_2 are the heat transfer coefficients of units 1 and 2.

In experiments for measuring the fabric heating rate, the fabric sandwich is heated from both sides with the thermocouple in between, or at the plane of symmetry; thus the heating rate expression is identical to the one of heating a fabric from one side while having the other side insulated and eq. (5) applies:

$$h_F = \frac{\rho_F' \cdot C_F}{t} \ln \frac{T_\infty - T_0}{T_\infty - T_M} \qquad \text{(5—Paper I)}$$

The same result is obtained by substituting for A_s in eq. (22) by $1/\rho_F'$.

In order to compare the heat transfer coefficients of the coloring processes under investigation (thermosol, HT steaming, and HTP), eq. (5) is applied to published data on fabric heating rates obtained using laboratory equipment simulating the three methods commonly used for coloring polyester. The comparison is based on the time ($t_{0.9}$) as in eq. (53). For the sake of simplicity, a lumped overall heat transfer coefficient has been assumed for HT steaming based on $t_{0.9}$. The steam condensation (during HT steaming) on the fabric and subsequent evaporation effects, then heating of the fabric to the ambient temperature are approximated by an "equivalent" continuous heat convection process.

The data compiled in Table IX cannot be used for determining the absolute values of the heat transfer coefficients because there is insufficient information for determining the fabric areal densities (ρ_F') of the samples used in the references of Table IX; however, the same fabric is used in each study for the comparative measurements of the heating rate, and thus the relative values of the heat transfer coefficients are meaningful. Table IX shows the similarity between the overall heating characteristics of units using superheated steam and air.

Figure 15 demonstrates the heating rate behavior during HTP of two polyester jersey fabrics from two different data sources: Gorondy,[6] curve 2 with T_∞ = 210°C, and Wakida et al.[8] curves 6, 7, and 8 at three different heat source temperatures: T_∞ = 230°C, 210°C, and 190°C, respectively. The experimental setup in both Refs. 6 and 8 is as follows: A thermocouple is placed on top of a heat insulating stand, then the fabric (0.214 kg/m^2 in Ref. 6 and 0.25 kg/m^2 in Ref. 8) is layed on the stand and covered with a transfer paper sheet, and then a hot plate at temperature T_∞ is lowered and contacted with the paper-fabric

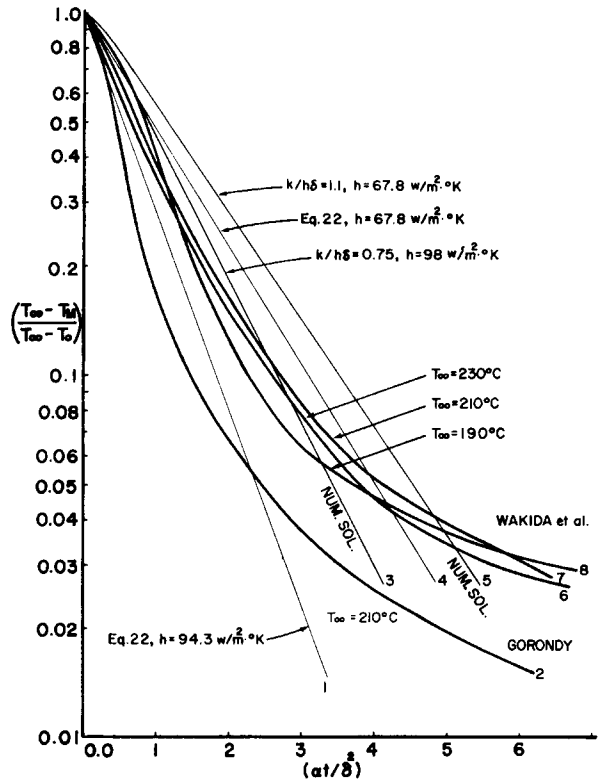

Fig. 15. Fabric heating behavior during heat transfer printing.

assembly with a pressure of about 10 kN/m^2 (1.5 psi g) in Ref. 6 and 11.7 kN/m^2 (1.7 psi g) in Ref. 8. The fabric is heated from one side and insulated from the other side, and the measured temperature becomes T_M, as discussed above.

Applying a mechanical pressure on the fabric surface—as during HTP—reduces the fabric thickness ($2\delta_F$), thereby increasing the fabric density. However, the fabric thickness is not only reduced due to the mechanical contact pressure, but also due to the thermal energy that softens the fiber in the fabric which leads to a transverse—across the fabric thickness—relaxation. Under a given mechanical contact pressure, the higher the temperature is, the greater will be the fabric thickness reduction, density, and, accordingly, stiffness.[8]

By extrapolating the data in Ref. 8 of the fabric thickness vs. load, the ($2\delta_F$) value obtained for the prevailing pressure (1.7 psi g) is 8.7×10^{-4} m for the untreated (not heat set) fabric; hence, $2\delta_F$ for the fabric used in Ref. 8 is assumed to be 8×10^{-4} m—thus taking into account the thermal treatment effect. Note that the $2\delta_F$ value is equivalent to δ in Figure 15 as a result of the heating symmetry in the fabric discussed earlier.

All the experimental heating rate curves in Figure 15 have two major characteristics: (1) a development of a convex (towards the ordinate) curvature such that the higher the hot plate temperature (T_∞) is, the earlier the convexity appears and develops; and (2) as the heating proceeds after the convexity formation, an additional reduction in the fabric heating rate is observed starting around T_M = 170°C. These two characteristics are obvious deviations of the fabric

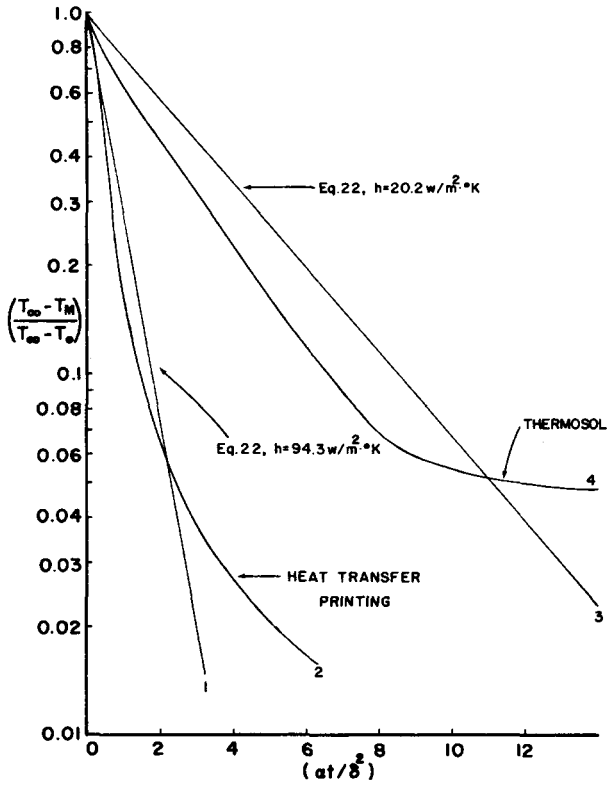

Fig. 16. Fabric heating rate during thermosoling and heat transfer printing; data from Gorondy.

heating rate from that of a homogeneous geometrically stable plate with constant thermal diffusivity and specific area of heat transfer (as assumed earlier in modelling the fabric heating), which should yield straight lines beyond the initial heating stage as in curves 1, 3, 4, and 5 of Figure 15.

Since the fabric is highly porous (about 80% of the fabric volume is air), a thickness reduction will initially improve the contact and decrease the air layer thickness between the individual fibers throughout the fabric cross section, thereby increasing the overall heat transfer coefficient to the fabric and consequently the fabric heating rate, which is manifested by the appearance of the convexity of the fabric heating curves in Figure 15. However, too much contact between the fibers in the fabric will result in a reduction of the real specific area of heat transfer to these fibers due to fiber aggregation. [Increasing a cylinder (fiber) diameter R_f reduces the cylinder specific heat transfer area ($A_f = 2/\rho_f \cdot R_f$) and increases the cylinder heating time to reach a given temperature.] The higher the hot plate temperature, the softer the individual fibers become and the easier the formation of "fiber aggregates" of larger diameters during the transverse relaxation, which explains the slowdown in the fabric heating rate in Figure 15.

When the fiber aggregation is compounded by the fiber increase in softness (specially at higher T_∞ values) and partial adherence, further aggregation of fibers becomes more and more difficult because of the more viscous (difficult) fiber flow (displacement) inside the fabric. As a result, the fabric compressibility is

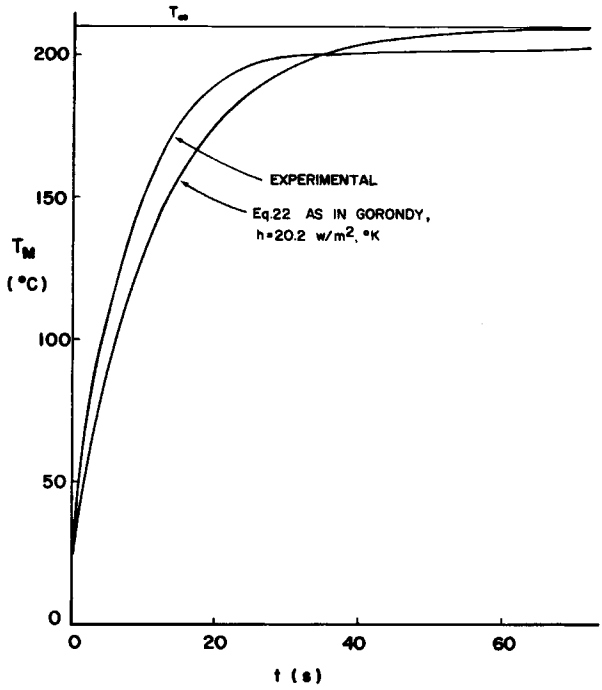

Fig. 17. Modelling of the jersey polyester fabric heating during thermosol.

relatively reduced. On the other hand, when this aggregation is not accompanied by severe fiber softening (the polyester fiber "softening point" is around 220°C[6]), the constant pressure and heat (at T_∞ = 190°C)—which trigger the transversal relaxation—cause the fibers in the fabric interior to continuously glide over one another and to assume positions resulting in more fabric compactness and aggregation; under such conditions the fabric air content is highly reduced. This results in a further decrease of the real specific heat transfer area of the geometries being heated by (1) direct contact with the hot plate at the fabric surface and (2) convection from the surrounding air in the fabric interstices that has—as will be shown later in Table XII—a thermal diffusivity that is orders of magnitude larger than that of the fiber and reaches T_∞ in a fraction of a second. A too compact fabric will force a large volume of this air out of the fabric structure.

In other words, decreasing the distance between the individual fibers in the air-filled fabric intersticies improves the heat transfer to the fibers. However, eliminating the air from the fabric interstices reduces the overall heat transmission process inside the fabric because of the elimination of the heat transport by convection within the fabric. This clarifies the significant reduction in the last portion of the heating rate curve 8 at T_∞ = 190°C in Figure 15.

Summarizing, curves 2, 6, 7, and 8 in Figure 15 manifest variations in both the overall heat transfer coefficient and the real specific area of heat transfer of the fabric as result of the fabric geometrical instability during the heating process.

Figure 16 illustrates the fabric heating rate during HTP and thermosol processes at T_∞ = 210°C. The thermocouple in the latter process is placed between two layers of the polyester fabric that are layed on a frame then placed in the

thermosol oven. Due to the lower overall heat transfer coefficient in thermosol, the initial heating rate in curve 4 is linear and both eq. (22) and the numerical analysis solutions can be made to fit this first portion of the curve—as discussed above and demonstrated in Figure 10. But, again, at around 200°C the heating rate declines sharply due to geometrical instabilities that result in the reduction of the real specific area of heat transfer to the fabric as for HTP.

The reason that curve 4 of Figure 16 manifests a more severe (than in HTP) slowdown in the heating rate of the jersey fabric is that under the thermosol conditions the fabric suffers a greater reduction in its thickness accompanied by a striking increase in the fabric stiffness.[8] This would be expected since the fabric can relax in both its thickness and its planar directions, and the fibers in the fabric interior are less restricted than during HTP. In thermosol, fixing the edges of the fabric to a frame does not inhibit the "fiber flow" in the planar direction of the fabric relative to having a continuous pressure acting over the fabric surface as in the case of HTP. The reduced restraint on the fiber movement in the fabric, and the lower heat transfer coefficient, result in a relatively easy and slow fiber aggregation that produces a fabric with a lower real specific area of heat transfer and accordingly a lower heating rate, as in curve 4 of Figure 16.

It is interesting to note that there is no convexity in curve 4 of Figure 16 as contrasted with HTP data curves of Figure 15. This is a consequence of the very low h value which is a characteristic of the thermosol heating, and the rate-determining step of the fabric heating during the linear portion of curve 4 is the heat transmission from outside to inside the fabric. During the final fabric heating stage, the reduction in the real specific area of heat transfer is so large such that the heat transport inside the fabric becomes the rate-determining step thereafter.

From the above it is clear that an exact modelling of the given fabric heating rate involving all the dimensional instabilities is an extremely complex matter. Figures 15 and 16 illustrate the usage of eq. (22) for representing the fabric heating rate by forcing the solution to converge at the point where $T_M = 200°C$ when $T_\infty = 210°C$, thereby determining an apparent overall heat transfer coefficient h. The advantage of eq. (22) in this case is that it does not involve more than one variable parameter since ρ_F and C_F remain practically unchanged. The numerical analysis solution assuming a constant (h) value and a fixed fabric thickness gives a poor fit, as illustrated in Figure 15 by curves 3 and 5. A better representation of the initial heating rate before the fabric relaxation at $T_\infty = 190°C$ can be made using the numerical solution as in curve 3, but this fitting can be easily matched by using eq. (22) and increasing the value of h.

The semilogarithmic plots in Figures 15 and 16 exaggerate the real deviation of the models from the data; for instance, a very poor agreement appears in the case of thermosol in Figure 16 curves 3 and 4. However, by replotting the two curves, as in Figure 17, a better agreement results which demonstrates the usefulness of the simple expression in eq. (22). Unless one uses a more sophisticated model that involves at least a variable fabric thickness and a heat transfer coefficient that embodies the effect of the fabric real specific heat transfer area, the numerical analysis solution (in this case) does not represent a viable alternative to eq. (22). Nevertheless, the semilogarithmic plots in Figures 15 and 16 are useful for demonstrating and analyzing the fabric heating deviation from the semiinfinite plate model.

TABLE X
Fabric Heating Rate During HTP and Thermosol

	HTP press[a]		Thermosol				
T_∞ (°C)	$t_{0.9}$ (s)	h_{HTP} (W/m^2·°K)	$t_{0.9}$ (s)	h_A (W/m^2·°K)	(h_{HTP}/h_A)	$(h_{HTP}/h_A)^b$	Ref.
210	7.5	94.3	35	20.2	5	10	6
210	15	67.8	—	—	—	—	8

[a] Pressure on fabric used in Ref. 6 is about 10 kN/m^2 (1.5 psi g) and in Ref. 8 11.7 kN/m^2 (1.7 psi), and ρ_F' is 0.214 and 0.250 kg/m^2 in Refs. 6 and 8, respectively.

[b] For continuous HTP operation, h_{HTP} was assumed to be double that of h_{HTP} for batch operation.

Table X summarizes the values of the heat transfer coefficients for HTP and thermosol as obtained from eq. (22) and Ref. 6 using the data in Refs. 6 and 8. The reason for the relatively lower h_{HTP} value in Ref. 8 relative to Ref. 6 is possibly due to the fact that in Ref. 6 the HTP press stand is preheated before inserting the fabric under the hot plate—the pressure and fabric used by both workers are similar. Nevertheless, the characteristics of the heating curves (as in Fig. 15) are the same.

High temperature steaming is known to produce a finished fabric with better hand properties (or less fiber aggregation) than either thermosol or HTP[9,13]; nevertheless, fabric relaxation under any high temperature treatment is inevitable. This implies that during HT steaming the real specific surface area of the fabric is not as severely reduced as during thermosol or HTP. Accordingly, it may be hypothesized that the water molecules in the superheated steam (during HT steaming) inhibit softened fiber adhesion and aggregation at the treatment temperature.

The assumption made in Table X of the value of h_{HTP} for the continuous HTP process is reasonable and is based on values of heat transfer coefficients for direct contact units as in Table VI. Thus, the heating efficiency in HTP is at least 10 times that of conventional thermosol units using hot flue ovens.

One concludes from Table IX and X that the heat transfer characteristics of thermosol (hot air) and HT steaming (superheated steam) are similar and that HTP produces by far the highest heat transfer coefficients (or heating rates). Table XI illustrates the similarity between the heat transfer parameters in superheated steam and air at the operating temperature range during thermofixation.

Meaning of the Fabric Temperature

Table XII shows the thermal properties of the polyester fiber, air, and the fabric ($\rho_F' = 0.24$ kg/m^2, $2\delta_F = 0.001$ m) at the arithmetic average temperature ($\overline{T}$) between $T_\infty = 200$°C and $T_0 = 20$°C: $\overline{T} = 110$°C.

From density values in Table XII, there is 0.83 m^3 of air associated with each m^3 of fabric, which explains the fabric reduction in thermal conductivity compared to a fiber. On the other hand, the fabric gains or loses heat more easily than the fiber—a result of an increase in the fabric thermal diffusivity due to the presence of air. Since the fabric is (volume-wise) 83% air, a thermocouple that is placed between two layers of fabric in order to measure the midplane temperature (T_M) will actually be measuring a certain "average" temperature

TABLE XI
Thermal Properties of Superheated Steam and Air at 180°C and 200°C (Ref. 2)

	Superheated steam[a]				Air[a]			
T (°C)	k	ρ	Cp	α	k	ρ	Cp	α
180	0.0348	0.484	1.975	3.6×10^{-5}	0.0378	0.755	1.021	5.0×10^{-5}
200	0.0365	0.464	1.975	4.0×10^{-5}	0.0393	0.722	1.025	5.3×10^{-5}

[a] k = thermal conductivity (W/m·°K), ρ = density (kg/m^3), Cp = specific heat capacity (kJ/kg·°K), α = thermal diffusivity (m^2/s).

of the fiber surfaces and air. However, the air in the fabric heats extremely rapidly due to its high thermal diffusivity compared to a fiber. The consequences of that are considered in the next section.

Air in the Fabric Interstices Heating Rate and Consequences in HTP

Heating a close, constant volume, air-filled fabric, as in the case of a large HTP press with rigid boundaries, will increase the air pressure inside the system. The ideal gas law is

$$PV = nRT \tag{54}$$

where P is the gas pressure, V the volume, n the number of moles present, R the ideal gas constant, and T the gas temperature (°K).

Thus, for a constant gas mass (n) and volume (V) eq. (54) gives

$$P_1/P_2 = T_1/T_2 \tag{55}$$

Accordingly heating up a gas (as air) in a closed volume from 20°C to 210°C will increase the gas pressure by 69 kN/m^2 (10 psi g) if the initial gas pressure is atmospheric or at 101 kN/m^2 (14.7 psi a). Due to the permeability of the blanket in continuous HTP, air can escape to the surrounding atmosphere. A blanket of low permeability can cause serious problems; at one extreme the blanket can be pushed away from the heating calender, since the blanket pressure usually does not exceed 13.8 kN/m^2 (2 psi g), as result of the pressured air (10 psi g) entrapped between the blanket and the surface of the calender. This will result in poor contact between the calender heating surface and the substrate being heated, thereby reducing the overall heating efficiency. In addition, a poor contact between the HTP sandwich components will decrease the friction between the moving fabric and HT paper, which can cause problems for the printed pattern registration. Assuming a heat transfer coefficient of 5 W/m^2 · °K for the natural convection of heat from the calender surface to the air, and an air slab thickness of 0.001 m, this air slab will heat from 25°C to 200°C in about 0.5

TABLE XII
Fabric and Fiber Thermal properties at 110°C

	k (W/m·°K)	ρ (kg/m^3)	C (kJ/kg·°K)	α (m^2/s)	Ref.
Fiber	0.163	1.38×10^3	1.67	0.7×10^{-7}	14
Air	0.0325	0.722	1.01	530×10^{-7}	1
Fabric[a]	0.064	0.24×10^3	1.38	2×10^{-7}	15

[a] For a 0.24 kg/m^2 fabric 0.001 m thick.

s. Similar results will be obtained by either using eq. (22) or the numerical analysis graphical solution as in Ref. 1 because of the high uniformity in the temperature distribution inside the slab. This is a consequence of the high thermal diffusivity of air as shown in Table XII. In thermosol or HT steaming the "air in the fabric" is not problematic.

SUMMARY

First it is shown how the numerical analysis solution can be degenerated to the simple body heating expression most commonly used in the textile literature [eq. (5)]. Then, an evaluation is made of the heat transfer coefficients (for different fabric heating equipment) as obtained from fabric heating rate measurements; and it is found that for high fabric heating efficiency equipment the reported h values are underestimated as result of using eq. (5) without recognizing its limitations in cases of large temperature nonuniformity in the fabric. Figure 13 illustrates the increase in the difference between the fabric surface temperature (T_S) and the fabric midplane temperature (T_M)—an indication of fabric heating nonuniformity—as the heat transfer coefficient from the heating source to the fabric is increased. Following is an analysis of the heat transmission to the individual fibers in the fabric. As a consequence of the relatively small exposure of the fibers to the heat source, the heat transfer coefficient to the fibers (h_f) is 1 or more order of magnitudes smaller than the heat transfer coefficient to the fabric surface (h_F)—as in Figure 14.

One concludes from the experimental results of the knitted polyester fabric heating rate that HTP provides the fastest heating of the fabric, whereas thermosol and HT steaming possess a similar overall heat transfer coefficient that is much lower than that for HTP. However, during the thermosol process, the fabric suffers more fiber aggregation and stiffness than HTP; during thermosol heating of the knitted fabric the individual fibers are not subject to much restraints (as in HTP) for lateral and across-the-fabric-thickness internal relaxation and consequent fiber adhesion type of aggregation, especially at high temperatures above 200°C. During HT steaming, the presence of the water molecules seems to inhibit the fiber's adhesion thus preserving the fabric hand properties. Finally, considering all the geometrical changes that occur during high temperature treatments of the polyester knitted fabric, the simple expression for representing the fabric heating [eq. (22) or (5)] is a practical and simple alternative to a sophisticated fabric heating model involving a heat transfer coefficient varying with the fabric temperature and the outside pressure as during HTP.

CONCLUSIONS

A clear distinction has to be made between evaluating the heat transfer coefficient of an equipment, and modeling the heating of a fabric. Evaluating the heat transfer coefficient of an equipment can be simply and correctly made by using a geometrically stable fabric that would approximate the homogeneous plate model. Whereas modelling a fabric heating may, for the sake of simplicity, involve an apparent heat transfer coefficient that is more dependent on the fabric characteristics and past thermal treatment history than the equipment efficiency in transmitting the thermal energy. As a result, different types of fabric with

different thermal history may produce a spectrum of values for the equipment heating efficiency. Therefore, it would be highly desirable to develop a standard methodology for estimating the heat transfer coefficient of heating equipment in the textile industry in order to be able to reliably communicate the heat transmission efficiency of the different types of heating units.

References

1. C. P. Kothandaraman and S. Subramanyan, *Heat and Mass Transfer Data* Book, 2nd ed., Wiley, New York, 1975.

2. R. H. Perry and C. H. Chilton, *Chemical Engineering Handbook*, 5th ed., McGraw-Hill, New York, 1973.

3. R. C. Weast, *Handbook of Chemistry and Physics*, 55th ed., CRC Press, Cleveland, Ohio, 1975, p. F114.

4. O. Stepanek, "Optimierung des Technologischen Verfahrens der Fixierung von Dispersionsfarbstoffen beim Druck von Polyesterfasern," *Veda Vyzk. Textiln. Prumysyl.*, **16,** 125 (1975).

5. H. Hauben and M. Pabst, "Thermosolage et Thermofixation sur les Machines a Cylindres," *Teintex*, No. 10, 519 (1974).

6. E. J. Gorondy, "Vapor Fixation of Disperse Dyes in Polyester," AATCC International Dyeing Symposium on Practical Dyeing Problems. Analysis and Solutions, Washington, D.C., May 25–26, 1977, p. 75.

7. S. Naka and Y. Kamata, "The Effect of Bulk Density on Thermal Conductivity of Fabrics," *Sen'i Gakkaishi*, **30**(2), T-43 (1974).

8. T. Wakida, T. Takagishi, T. Oshima, and N. Kuraki, "Setting Effects of Polyester Fabrics Treated by Heat Transfer Printing," *Sen'i Gakkaishi*, **32**(10), T-345 (1976).

9. R. T. Norris, "High Temperature Steaming in Continuous Piece Goods Dyeing," *Text. Chem. Colorists*, **1**, 88 (1969).

10. L. W. C. Miles, "Dye Fixation with Steam," *Ciba-Geigy Rev.*, No. 2, 18 (1974).

11. S. Mackawa, "High Temperature Steaming Process of Polyester Fiber with Disperse Dyes," *Jpn. Text. News*, No. 250, 111 (1975).

12. A. P. Lockett, "Some Possibilities of High-Temperature Steaming in Textile Printing," *J. Soc. Dyers Colourists*, **83,** 213 (1967).

13. M. R. Fox, W. J. Marshall, and N. D. Stewart, "Padding, Drying, Steaming and Baking Stages in the Application of Dyes to Cellulose Fibers and their Blends with Polyester Fibers," *J. Soc. Dyers Colourists*, **83,** 493 (1967).

14. S. Naka and Y. Kamata, "Measurement of The Thermal Conductivity of Fiber Perpendicular to its Axis," *Sen'i Gakkaishi*, **26**(3), T-43 (1973).

15. S. Baker, G. G. Tesoro, T. Y. Toong, and N. A. Moussa, *Textile Fabric Flammability*, MIT Press, Cambridge, Mass., 1976.

16. S. E. Akaoui, *J. Appl. Polym. Sci.*, **27,** 4693 (1982).

Received October 9, 1981
Accepted June 24, 1982